ELSEVIER

Chemical Engineering Journal 84 (2001) 31–41

Chemical Engineering Journal

www.elsevier.com/locate/cej

Phase transitions in a bed of vanadium catalyst for sulfuric acid production: experiment and modeling

B.S. Bal'zhinimaev*, N.P. Belyaeva, S.I. Reshetnikov, E.S. Yudina, A.A. Ivanov

Boreskov Institute of Catalysis, Russian Academy of Sciences, Pr. Lavrentieva 5, Novosibirsk 630090, Russia

Received 4 January 2000; accepted 21 June 2000

Abstract

Sulfur dioxide oxidation on vanadium catalysts in sulfuric acid production may cause phase transitions in the catalyst active component. These phase transitions involve crystallization of vanadium(IV), and may influence catalyst activity. In the present study, we show that reaction mixture flow through a fixed catalyst bed is accompanied by the moving front of crystal phase, which decreases SO_2 conversion at reactor outlet. Front profile and its movement velocity depend on the chemical composition of active component, support porous structure, catalyst particle size, and other parameters. Based on the Gibbs–Volmer theory, we suggest a simplified mathematical model, which (qualitatively and quantitatively) describes experimentally observed dynamics of front generation and movement, as well as related changes in the bed activity. The model allows us to predict catalyst behavior in an industrial scale reactor, and to optimize catalyst properties.

Keywords: Phase transitions; Vanadium catalysts; Gibbs–Volmer theory; Mathematical modeling

1. Introduction

Since the early 1930s, sulfuric acid production has been based on SO_2 oxidation to SO_3 over vanadium catalysts. Despite continuing attention to this reaction for many years, researchers could not explain and thus predict some specific reaction phenomena such as

- a sharp decrease of catalyst activity at a low sulfur dioxide conversion [1,2];
- a sharp change of the Arrhenius dependence at low temperatures [3];
- activity hysteresis with respect to conversion and temperature [4–6].

Note that SO_2 oxidation to SO_3 over vanadium catalysts accompanies some other industrial processes such as $DeNO_x$ with ammonia or regeneration of cracking catalysts [7,8]. However, the above-mentioned phenomena are inherent solely in the catalysts for sulfuric acid production. The reason is that under reaction conditions, the catalyst active component is a melt, and reaction goes on in the bulk of this melt.

Studies performed at the Institute of Catalysis and focused on the active component performance, reaction mechanism, and catalyst state in situ, unambiguously show that all phenomena we are concerned with are related to phase transitions, occurring in the active component. These phase transitions involve crystallization of species of vanadium(IV) [6].

Active component melt is represented by the system $M_2S_2O_7$–M_2SO_4–V_2O_5, where alkaline admixtures M (M = K, Na, Cs) act as promoter. In accordance with the detailed reaction mechanism [9], the catalytic cycle occurs in the coordination sphere of binuclear complexes of vanadium(V). However, there is a side process, which yields reduced vanadium species, which are mostly vanadium(IV). The reaction mechanism may be schematically presented as follows:

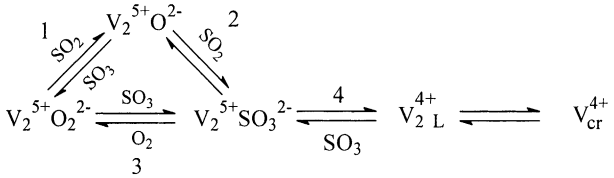

(1)

At low temperature and conversion vanadium(IV) content in the melt Θ_L becomes so high that vanadium(IV) crystallizes into a separate phase V_{cr}^{4+}. Crystal phase vanadium does not participate in the main reaction, so catalyst activity decreases. As reaction temperature (or SO_3 content)

* Corresponding author. Tel.: +7-3832-344770; fax: +7-3832-343766.
E-mail address: balzh@catalysis.nsk.su (B.S. Bal'zhinimaev).

1385-8947/01/$ – see front matter
PII: S1385-8947(00)00262-X

Nomenclature

c, C	molar portions of SO_2 inside catalyst grain and on its surface
D_{eff}	apparent coefficient of reagents diffusion in the gas phase inside the catalyst grain
D_v	diffusion coefficient
g	geometry factor
k	Boltzmann constant
N_0	number of vanadium atoms
r	radius reduced to spherical crystal size
Δr	diffusion layer thickness
$\bar{r}$	relative pore radius expressed as r/r_p
r_0	radius of binuclear vanadium complex
r_{cr}	critical nucleus size
r_p	radius of support pores
r^*	over critical radius of crystal phase nucleus
$\bar{r}^*$	critical nucleus radius ratio to pore radius
R_{ef}	apparent radius of catalyst grain
S	supersaturation
T	temperature (K)
v_0	molecular volume
V_L	melt volume
W	reaction rate in the catalyst grain (cm^3/g_{cat} s)
W_s	reaction rate on the catalyst grain surface (cm^2/g_{cat} s)

Greek symbols

γ	bulk density of catalyst bed (g/cm^3)
γ_{cat}	catalyst specific weight (g/cm^3)
δ	vanadium portion in crystal phase
η	effectiveness factor
Θ_{eq}	equilibrium concentration of $V_L{}^{4+}$
Θ_L	content of V^{4+} in liquid phase ($molecules/cm^3$)
Θ_∞	solubility of compounds V^{4+} in the melt
λ	specific heat evolution (grad)
ξ	dimensionless coordinate along reactor
ρ	dimensionless coordinate of grain radius
σ	interface energy
τ	conditional residence time (s)
ϕ	edge wetting angle
φ	modified Tiele module
Ω	frequency factor

increases, the crystal phase partially or completely dissolves, depending on reaction conditions.

As reported in [10], the crystallization process is the reason for catalyst activity decrease in the low temperature zones in industrial apparatuses (in particular at the second stage of a two-stage contact), and this essentially reduces catalyst operation life. Therefore, phase transitions in the active component of catalysts for sulfuric acid production are of both practical and theoretical interest.

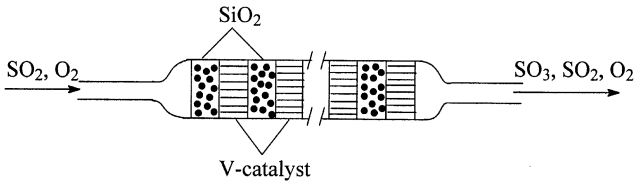

Fig. 1. Schematic diagram of isothermal plug flow reactor.

In the present study, we consider the influence of phase transitions involving vanadium(IV) on the fixed catalyst bed activity. We also suggest a mathematical model, describing the dynamics of phase transition in the catalyst bed.

2. Experimental

Phase transitions were studied in a fixed bed reactor represented by a glass tube 5.1 mm in diameter and 100 mm long (see Fig. 1). Catalyst consisted of 0.1–1.0 mm grains (kinetic regime) or cylinders (5 × 5, mm; industrial type, inner diffusion regime). For isothermal conditions, the catalyst sample (0.5–1.0 g) was divided into 8–10 equal parts to be separated by inert heat carrier particles of the same size: crushed quartz (0.5–1.0 mm) or silica cylinders (5 × 5, mm).

Reaction mixture containing SO_2 and oxygen in helium was supplied into the reactor preheated with air. We followed the SO_2 conversion at the reactor outlet, starting and outlet mixture being analyzed with GC. Starting mixture composition was 1% SO_2, 4.5% O_2, balance helium. The only exception was an experiment presented in Fig. 2, when the starting reaction mixture contained 0.25% SO_2, 2.5% O_2, balance He. In all experiments, reaction temperature was 693 K.

At a certain moment, the reactor was isolated, and quickly cooled to room temperature. In each section of catalyst bed, we determined the amount of V(IV) in the crystal phase. In order to obtain information on the dynamics of the crystal phase front along the catalyst bed, we repeated the experiments, varying time on stream, other conditions being the same.

Each section of catalyst (small or larger fraction) was thoroughly ground and mixed for averaging. ESR was used to determine the amount of V^{4+} in the crystal phase. The ESR spectrum of V^{4+} in the crystal phase is represented by a single line, and its intensity serves to determine the amount of $V_{cr}{}^{4+}$ [1,11]. Spectra were recorded with ER 200D "Bruker".

According to [11], the close environment of a paramagnetic ion is preserved under quick cooling. Special experiments in the high temperature cell show that line shape and width remain the same. Singlet signal intensity, corrected for q-factor and temperature, also remains the same. Therefore, one may conclude that the crystal phase amount measured at room temperature quantitatively corresponds to that existing under reaction conditions.

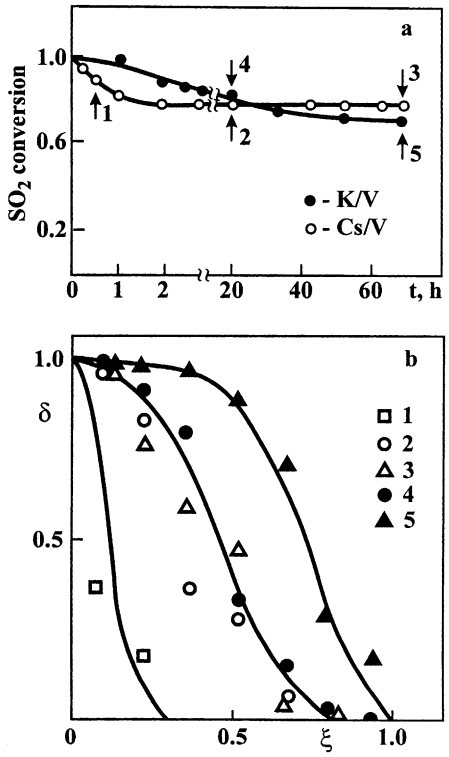

Fig. 2. Time dependence of SO_2 conversion (a) and crystalline phase amount δ vs. catalyst bed length ξ at moments marked by an arrow (b). Samples 1 ($\tau = 0.3$ s) and 5 ($\tau = 0.12$ s); catalyst fraction 0.5–1.0 mm; feed gas: 0.25% SO_2, 2.5% O_2 and He for balance.

All catalyst samples contained the same vanadium quantity equal to 7.5 ± 0.1 wt.% (see Table 1). We varied potassium to vanadium atomic ratio (K/V), and silica support pore size. In sample 5, cesium was introduced instead of potassium. Silica support of a bi-disperse structure was used to prepare samples 1 and 5, which contained mostly fine pores with a radius of 10 nm.

Typical experimental results are shown in Fig. 2. They were obtained with samples 1 and 5. Fig. 2a shows how SO_2 conversion at reactor outlet depends on time. Fig. 2b gives V^{4+} distribution over the whole catalyst bed at time moments shown with arrows. In this figure as well as in the next ones, the crystal phase distribution over the bed is given in coordinates $\delta(\xi)$, where ξ is a dimensionless coordinate over the reactor length, and $\delta(\xi)$ is determined as a ratio of singlet signal amplitude to its amplitude at the front bed ($\xi = 0$), where conversion is close to zero and thus almost all vanadium stays in the crystal phase.

Table 1
Properties of studied catalysts

Sample	M	M/V	Support pores radius, r_p (nm)
1	K	2.7	$r_1 = 10, r_2 = 400$
2	K	6	500–1000
3	K	2.7	500–1000
4	K	6	50–80
5	Cs	3	$r_1 = 10, r_2 = 400$

According to the figure, reaction mixture flows through the catalyst bed generates a crystal phase front, which with time moves through the bed. This transfer is accompanied by conversion decrease. Experiment shows the transfer rate to change with time. At the beginning it is fast, then it gradually decelerates, and at last the front stops. Since the front position becomes static, conversion becomes constant in time.

We observe visually how catalyst color changes from green at reactor inlet (high degree of vanadium reduction) to yellow at reactor outlet (most vanadium has valence 5).

2.1. Effect of active component chemical composition

Fig. 3 demonstrates the character of bed activity evolution with time, and crystal front positions at time moments shown with arrows for samples 2 and 3 differing solely in the ratio K/V. Experiments show that in sample 3 (K/V = 2.7) in 1 h vanadium is crystallized over the whole bed, while in sample 2 (K/V = 6) only half of the catalyst is crystallized in 3 h. Note that as ratio K/V increases, front transfer inside the catalyst bed decelerates.

The promoter also influences the crystal phase front dynamics. According to experimental data shown in Fig. 2, samples promoted with cesium are crystallized to less extent than those promoted with potassium. In the Cs-containing

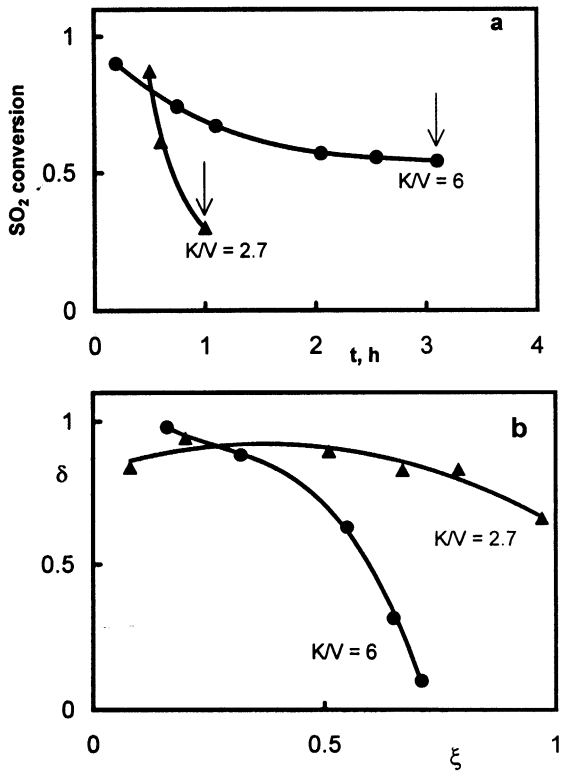

Fig. 3. Time dependence of SO_2 conversion (a) and crystalline phase amount δ vs. catalyst bed length ξ at time moments marked by an arrow (b). Samples differ by K/V ratio: 6 (sample 2, $\tau = 0.6$ s), 2.7 (sample 3, $\tau = 1.6$ s); catalyst fraction 0.5–1.0 mm.

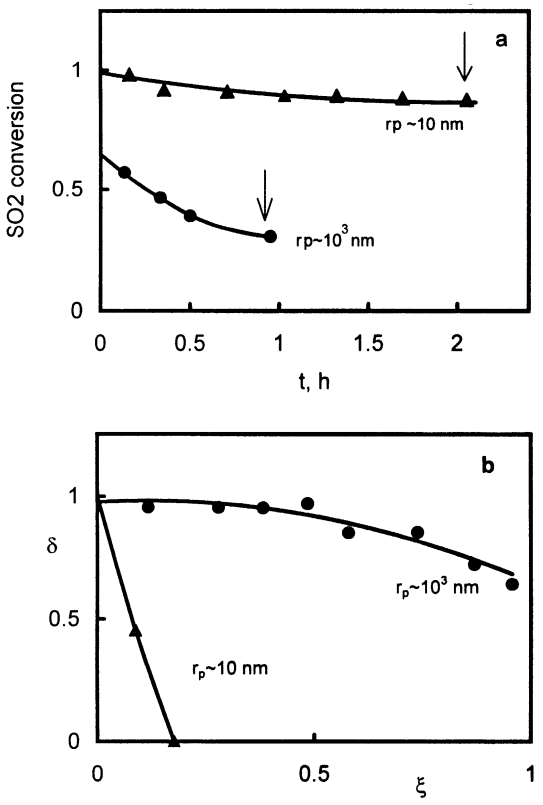

Fig. 4. Time dependence of SO_2 conversion (a) and crystalline phase amount δ vs. catalyst bed length ξ at time moments marked by an arrow (b). Samples differ by pore radii of support: 10 and 1000 nm. $\tau = 0.5$ s; catalyst fraction 0.5–1.0 mm.

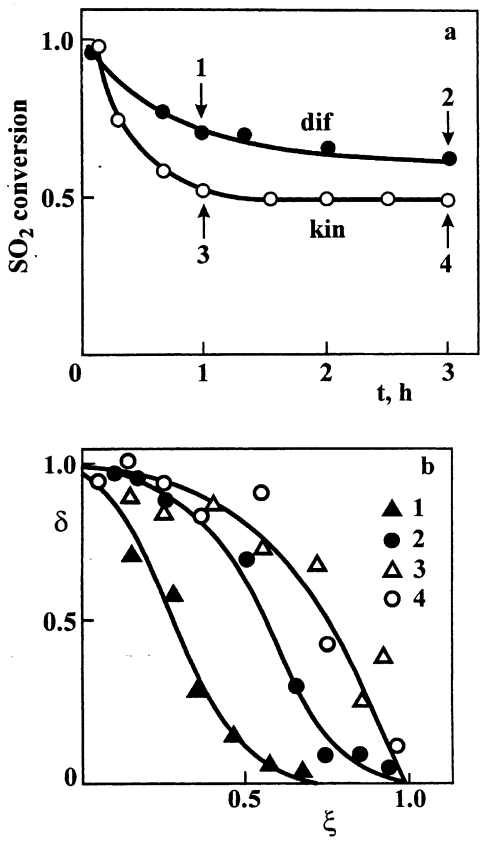

Fig. 5. Time dependence of SO_2 conversion (a) and crystalline phase amount δ vs. catalyst bed length ξ at time moments marked by an arrow (b). Particles of sample 2 differ by size: 5×5, mm (1, 2) and 0.5–1.0 mm (3, 4). $\tau = 0.6$ s.

sample, the front stops rather quickly, and thus catalyst bed activity is stabilized. In the bed of K-containing sample, the front moves during the whole run.

2.2. Effect of support porous structure

Support porous structure also has an essential influence on the crystal phase front dynamics (see Fig. 4, samples 1 and 3). At the same residence time, almost all vanadium changes to a crystalline state in 1 h on the support with wide pores (500–1000 nm). When the support has fine pores (pore radius 10 nm), after 2 h the front is still localized near the bed inlet.

2.3. Catalyst particle size effect

Front movement peculiarities become even more complex, if reaction occurs over the large catalyst particles, when SO_2 oxidation is governed by the inner diffusion regime. Experiments with small particles (0.5–1.0 mm) and large particles (5×5, mm) (see Fig. 5) show that with small particles the crystal phase front transfers inside the bed faster than with large particles. Thus, we have a paradox: sample activity under the kinetic regime is lower than under the inner diffusion regime.

2.4. Prehistory effect

Experiment with sample 1 is of interest (see Fig. 6). When we supply the reaction mixture with the flow rate of 1.6 cm^3/s onto the oxidized sample, we observe some decrease of catalyst activity leading to a quasi-stationary conversion $X_1 = 0.86$. As flow rate increases to 2.3 cm^3/s, conversion decreases to $X_2 = 0.76$. If onto the oxidized sample we supply reaction mixture with a 2.3 cm^3/s flow rate, then conversion stabilizes at $X_3 = 0.68$. This value is noticeably lower than the one we obtain with a stepwise flow rate increase. Conversion values are in agreement with the crystal phase front position. The deeper the front inside the bed, the lower the conversion at the outlet. Experiment shows that final front position (and thus quasi-stationary catalyst activity) depends not only on reaction conditions, but also on the prehistory of events.

Generalizing experimental results, we may conclude that many factors affect the crystallization dynamics, the front profile, its movement along the bed, and catalyst deactivation. Among these factors are:

- catalyst chemical composition;
- support porous structure;

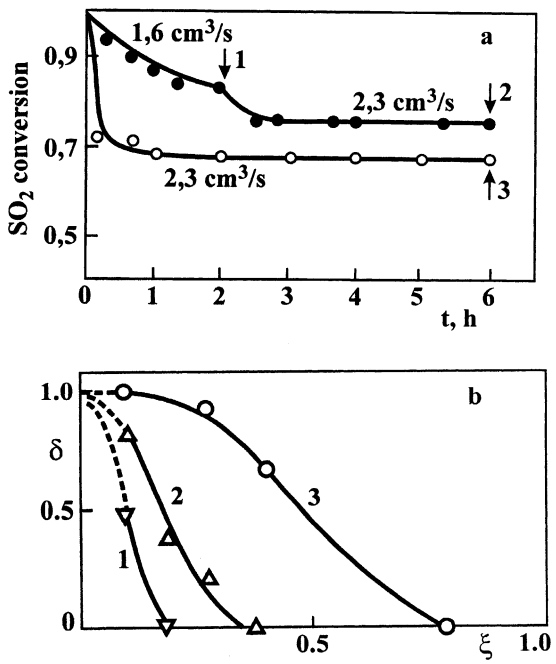

Fig. 6. Time dependence of SO_2 conversions (a) and crystalline phase amount δ vs. catalyst bed length ξ at time moments marked by an arrow (b). Sample 1, fraction 0.5–1.0 mm, weight: 0.5 g. Volume velocity: 1.6 cm^3/s (1) and 2.3 cm^3/s (2, 3).

- catalyst particle size;
- prehistory of events occurring in the catalyst bed.

We may also add such factors as SO_2 concentration in the inlet gas mixture. Vanadium content in the crystal phase increases as SO_2 concentration grows.

3. Kinetic model for phase transition dynamics

Our kinetic model is based on the classic theory of phase transitions — the Gibbs–Volmer–Zeldovitch theory. According to the theory, the crystallization process involves such stages as new phase nuclei generation, and their growth to macroscopic size through primary and secondary crystallization. Supersaturation S is necessary for the critical nuclei generation in the solution. Factor S is determined as a ratio of the current concentration to equilibrium one for the dissolved substance.

Critical solution, which precedes the generation of nuclei, is an oversaturated or metastable liquid. Metastable state life strongly depends on factor S or in other words on the height of the free energy barrier required for a critical nucleus to form (ΔG_{cr}). Nuclei generation rate I and critical nucleus size r_{cr} are determined by the following expressions [12,13]:

$$I = \Omega \exp\left(\frac{\Delta G_{cr}}{kT}\right) = \Omega \exp\left(\frac{-g v_0^2 \sigma^3}{(kT)^3 \ln^2 S}\right) \quad (2)$$

$$r_{cr} = \frac{2\sigma v_0}{kT \ln S} \quad (3)$$

where Ω is the frequency factor, g the geometry factor (for spherical nuclei $g = \frac{16}{3}\pi$), v_0 the molecular volume, σ the interface free energy, k the Boltzmann constant, and T the temperature.

New phase generation rate depends on many factors, which may be of a random character. For example, crystals may grow by the addition of V^{4+} complexes to smaller crystals or through agglomeration of several smaller crystals. As a whole, crystallization is complicated since some crystals are destroyed when they collide with each other.

In order to describe the dynamics of crystallization occurring in the liquid bulk, one uses a model including material balance for the crystallizing matter and an equation for the crystal size distribution [14].

From the mathematical point of view, this problem is reduced to the solution of an equation in partial derivatives, which describes the evolution of crystal size distribution in subsequent generations.

For our system, which is a vanadium catalyst for SO_2 oxidation, the supersaturation factor is determined by the ratio of V^{4+} concentration in the active component melt Θ_L to its solubility Θ_∞:

$$S = \frac{\Theta_L}{\Theta_\infty} \quad (4)$$

Value Θ_L, and thus supersaturation S, depends on the process performance conditions such as concentration of reagents and temperature. When we consider processes going in the catalyst bed, we must take into account how concentrations change along the bed, and over the radius of catalyst particles. Therefore, beside material balance for the crystallizing substance and crystal size distribution, the mathematical model for phase transition dynamics in the catalyst bed should also include equations which describe the diffusion processes in the particle and evolution of concentrations in the bed. Thus, even in the simplest case, if one considers the elementary volume of melt with a uniform supersaturation [15], there are many obstacles related to the calculation of the distribution density function.

For problem simplification we accepted the following assumptions:

1. all new phase nuclei appear simultaneously;
2. nuclei growth is limited by the diffusion of complexes V^{4+} in the melt;
3. nuclei are spherical.

The first assumption means that all nuclei grow in the same manner. In elementary liquid volume nuclei are of the same size at each time moment. This assumption is well grounded, if nuclei generation rate is high, as occurs at $S \gg 1$. Such supersaturation is rather typical for the active component melt at low temperature and low conversion.

The second assumption is related to melt representation as a viscous liquid with a very low mobility of vanadium complexes [16]. Their diffusion coefficient is $D_v \sim 10^{-8}$ cm^2/s

[9]. Therefore, we may use the Nernst equation to describe the rate of crystal growth [17]:

$$\frac{\mathrm{d}r}{\mathrm{d}t} = \frac{(\Theta_\mathrm{L} - \Theta_\mathrm{eq}) D_\mathrm{v} v_0}{\Delta r} \tag{5}$$

where Θ_eq is the equilibrium concentration of $V_L{}^{4+}$ at a given r, Δr the thickness of diffusion layer at the crystal surface. Value Θ_eq in the melt is determined by the Gibbs–Thompson equation:

$$\Theta_\mathrm{eq} = \Theta_\infty \exp\left(\frac{2\sigma v_0}{kTr}\right) \tag{6}$$

In this case, r in Eq. (5) is understood as some crystal radius reduced to spherical shape. The situation when $\mathrm{d}r/\mathrm{d}t = 0$ corresponds to the quasi-equilibrium system state, which tends to the true equilibrium at $r \to \infty$.

Chemical reaction rate far exceeds the rate of phase transition, as is shown in [18] giving rate constants for the stages of mechanism (1). Therefore, during crystal phase growth V^{5+} ratio to V^{4+} is maintained at some quasi-equilibrium value determined by temperature and conversion. In this case, vanadium(IV) content in the liquid phase is determined by the formula:

$$\Theta_\mathrm{L} = (1-\delta) F \frac{N_0}{N_\mathrm{L}},$$
$$F = \left[1 + \frac{k_{-4}}{k_4} P_3 \left(1 + \frac{k_{-2}}{k_4} + \frac{k_3 P_2}{k_2 P_1}\right)\right]^{-1} \tag{7}$$

where δ is the vanadium portion in the solid phase at the current time moment (ratio of the number of vanadium atoms in the crystal phase to total number N_0), V_L the volume of active component melt, F a kinetic expression determined by reaction mechanism (1) and governing the quasi-stationary state (portion) of reduced vanadium in the melt.

Since the active component melt does not stay in one pool, but is distributed over the support pores, then the walls of the support pores are a natural obstacle for crystal growth. Influence of support pore size on the crystallization process was well demonstrated in a previous study [19]. At the same chemical composition of catalysts and under the same reaction conditions the crystal phase quantity is lower the smaller are the support pores.

Let us introduce the dimensionless crystal radius $\bar{r}$, and express it through support pore radius r_p as $\bar{r} = r/r_\mathrm{p}$. Placing Eqs. (6) and (7) into (5), we obtain the equation for crystal growth:

$$\frac{\mathrm{d}\bar{r}}{\mathrm{d}t} = \alpha_\mathrm{D}\left(F(1-\delta)\frac{N_0}{V_\mathrm{L}} - \alpha_\infty \mathrm{e}^{\beta/\bar{r}}\right) \tag{8}$$

where $\alpha_\mathrm{D} = D_\mathrm{v} v_0 N_0/\Delta r V_\mathrm{L} r_\mathrm{p}$, $\beta = 2\sigma v_0/kTr_\mathrm{p}$, $\alpha_\infty = \theta_\infty V_\mathrm{L}/N_0$, V_L is the liquid phase volume, N_0 the total number of vanadium atoms, determined by vanadium concentration (usually 7–8 wt.% with respect to V_2O_5) and sample weight.

Designating the number of solid phase nuclei as n, and radius of vanadium monomer as r_0, let us express vanadium portion in the crystal phase as

$$\delta = \frac{\bar{r}^3 (r_\mathrm{p}/r_0)^3 n}{N_0} \tag{9}$$

We might have determined the number of forming new phase nuclei with formula (2), but we do not know the frequency factor entering this formula. In practice, it is very hard to measure the rate of nuclei generation, since at high supersaturation this process goes with a high rate. The largest number of nuclei n_max occurs at the maximum supersaturation S_max. Value n_max is estimated from experimental electron microscopy data as 10^{15}–10^{16} nuclei/cm^3. Under condition that all nuclei form simultaneously and grow independently (i.e. there is no nuclei distribution by size), nuclei number is proportional to the rate of nuclei generation, and thus $n \sim I(S)$. Their number is maximum at the maximum supersaturation $n_\mathrm{max} = I(S_\mathrm{max})$. Introducing n_max and S_max into (2) we obtain an equation determining the number of nuclei formed at supersaturation S:

$$n = n_\mathrm{max} \exp\left(-b\frac{\ln^2 S_\mathrm{max} - \ln^2 S}{\ln^2 S_\mathrm{max} \ln^2 S}\right) \tag{10}$$

where $b = \frac{16}{3}\pi\sigma^3 v_0^2/(kT)^3$.

The new phase nuclei generation process is of a random character, and goes with free energy ΔG, which attains a maximum for the nuclei of critical size. The energy maximum condition coincides with the equilibrium between the crystal and oversaturated liquid around it. However, this equilibrium is not stable: a growing nucleus turns into a crystal particle, but the nucleus may also dissolve if it decreases in size. Therefore, only those nuclei that have a size larger than the critical one, and whose free energy only differs by kT from the maximum energy, are able to survive in the process [14].

Eqs. (2) and (10) are true under the assumption that nuclei generation is homogeneous. In the real catalyst for sulfuric acid production large liquid–solid interface may essentially decrease the free energy for nucleus generation according to classical theory [20]. In the simplest case, the heterogeneity condition for a spherical nucleus may be expressed as

$$\Psi = \tfrac{1}{4}(1-\cos\phi)^2(2-\cos\phi), \qquad \Delta G_\mathrm{cr}^\mathrm{het} = \Delta G_\mathrm{cr}^\mathrm{hom}\Psi(\phi)$$

where ϕ is the edge wetting angle, ΔG^het and ΔG^hom stand for the free energy of nuclei generation with and without interface. Value $\Psi(\phi)$, depending on the wetting angle, may be much less than unity. Active component melt is well wetting silica surface, and thus the support micropores are essentially filled. According to [21], the wetting angle may attain several degrees. Therefore, over the interface, the free energy for nuclei generation may reduce by several orders of magnitude. Since wetting depends on many factors such as reaction mixture composition, temperature, admixtures,

one can hardly determine it experimentally. Therefore, the value of $\Psi(\phi)$ is adjusted for the possible best agreement between calculation and experiment. For this purpose, the value of b in (10) is multiplied by $\Psi(\phi)$.

Starting condition for Eq. (8) is written as

$$t = 0: \quad \bar{r} = \bar{r}^* \tag{11}$$

where $\bar{r}^*$ is the ratio of overcritical nucleus radius r to the pore radius. Number of nuclei with overcritical size is determined by formula (10), and the value r^* follows from the solution [12] of equation:

$$\Delta G = \Delta G_{cr} - kT \tag{12}$$

Condition ΔG corresponds to non-zero root

$$r_1 = \frac{3v_0\sigma}{kT \ln S}$$

Comparing value r_1 with r_{cr} in formula (3), we may write

$$r_{cr} < r^* < \tfrac{3}{2} r_{cr}$$

Numerical solution of Eq. (12) gives the radius of the critical size nucleus.

Therefore, under an assumption that new phase nuclei are spherical and of the same size we obtain Eq. (8) including Eqs. (9) and (10) with boundary conditions (11). Eq. (8) describes the growth of the crystal phase at the stage of primary crystallization.

4. Estimation of model parameters

Kinetic and physical–chemical methods such as NMR, ESR and HREM were used to estimate the main parameters that characterize the growth of new phase nuclei, and enter Eq. (8). Thus, according to NMR data [16] and kinetic experiment [20], the size of vanadium binuclear complex r_0 ($v_0 = \frac{4}{3}\pi r_0^3$) is 10^{-8}–10^{-7} cm. The value of Θ_∞ is estimated in [19] from the ESR spectra at $T = 693$ K as $\sim 10^{19}$ of binuclear vanadium complexes in 1 cm^3 of melt. This corresponds to 0.005 of the total vanadium amount N_0 ($N_0 = 2.4 \times 10^{20}$ V particles per gram). Kinetic experiments on the dissolving of crystal vanadium(IV) provided for the experimental value v_0 and Θ_∞ and for $\sigma = 10^{-5}$ J/cm^2, allow the estimation of other parameters. $D_v/\Delta r$ at 693 K is 10^{-8} cm/s, $E_{D_v/\Delta r} = 120$ kJ/mol, and dissolving heat $q = 20$–40 kJ/mol [17].

Based on the above given parameter estimates, we modeled phase transitions such as generation and dissolving of crystal species of vanadium(IV) for a single catalyst particle in the kinetic regime. Processing experimental data from [17] with model (8)–(11), we revised our values for the parameters. According to Table 2, values obtained with modeling are similar to those estimated using physical methods. Values $D_v/\Delta r$ and α_∞ are given at $T = 693$ K. Their activation energy and heat are equal to 83.6 and 62.7 kJ/mol, respectively.

Table 2
Parameters of kinetic model for phase transitions

Parameter	Experimental estimate	Value calculated with model
r_0 (cm)	10^{-8}–10^{-7}	0.6×10^{-7}
σ (J/cm^2)	10^{-5}	1.65×10^{-5}
$D_v/\Delta r$ (cm/s)	10^{-8}	3.0×10^{-8}
α_∞	0.005	0.0083
n_{max} (nuclei/cm^3 melt)	10^{15}–10^{16}	1.2×10^{16}
$\Psi(\phi)$	–	0.4×10^{-2}

5. Phase transitions in the catalyst bed

In order to describe phase transitions in the catalyst bed, we must expand set (8)–(11) with other equations following the changing reaction mixture composition both along the reactor and over the catalyst particle radius. The full mathematical model is written as

$$\frac{dC}{d\tau} = W(T, \vec{C})\gamma\eta \tag{13}$$

$$T = T_0 - \frac{\lambda(C - C_0)}{C_0} \tag{14}$$

$$\frac{1}{\rho^2}\frac{d}{d\rho}\left(\rho^2 \frac{dc}{d\rho}\right) = \frac{\varphi^2 W(T, \vec{c}, \delta)}{W_s(T, \vec{C})} \tag{15}$$

$$\frac{d\bar{r}}{dt} = \alpha_D \left(\frac{(1-\delta)N_0/V_L}{1 + (k_{-4}/k_4)P_3(1 + (k_{-2}/k_2P_3) + (k_3P_2/k_2P_1))} - \alpha_\infty e^{\beta/\bar{r}} \right) \tag{16}$$

with the following starting and boundary conditions:

$$t = 0: \quad \bar{r} = \bar{r}^*, \qquad \tau = 0: \quad C = C_0, T = T_0,$$
$$\rho = 0: \quad \frac{dc}{d\rho} = 0, \qquad \rho = 1: \quad c = C \tag{17}$$

where $\eta = \int_0^1 \rho^2 W(\bar{c}, T, \delta)/W_s(\bar{C}, T, \delta)d\rho$.

Reaction rate is determined from the kinetic equation

$$W = \frac{k_3' K_2 P_1 P_2}{1 + K_2 P_1 + K_3' P_2} \frac{1 - P_3^2/P_1^2 P_2 K_{eq}^2}{1 + aP_3}(1 - \delta) \tag{18}$$

Eq. (18) is presented in [21] as derived from mechanism (1). As we have already mentioned rate constants for reaction stages are given in [18].

This model differs from the usually applied one by Eq. (16), which describes the new phase nuclei growth. Since crystallization process is slower than inner diffusion, there is no time derivative in Eqs. (13) and (15).

6. Discussion

We consider how our experimental results may be explained with the Gibbs–Volmer theory, and how they agree with the calculations via above-described model.

As the reaction mixture passes through the catalyst bed, its composition along the reactor changes. With the growing conversion, V^{4+} content in the melt decreases, and so does supersaturation S. Fig. 7 shows how supersaturation changes with reactor length at different time moments regarding phase transitions going in the catalyst. Starting profile (curve 1) at $t = 0$ corresponds to the situation when there is no crystal phase. In the inlet layers, where $X \sim 0$, supersaturation and thus nuclei generation rate attain their maximum values. Therefore, supersaturation is quickly removed owing to a simultaneous generation and growth of a large number of relatively small ($r \sim 4$ nm) nuclei. To an order of magnitude the time of nuclei growth (and thus the time of supersaturation removal) is equal to r/α_D ($\alpha_D \sim 10^{-8}$ cm/s), and for $r \sim 10$ nm it is ~100 s. In this time, almost all vanadium in the inlet layers undergo a transition to crystal phase. In the next layers (owing to lower S) nuclei numbers sharply decrease. For supersaturation reduction, nuclei must grow to a larger size than in the previous layers. As a result, crystallization along the reactor decelerates, and a crystal phase front forms, whose profile is rather sharp. As inlet layers are deactivated, conversion over each cross-section decreases, and thus S in the following layers increases. Therefore, new nuclei intensively appear and grow, and S increases in the deeper layers. However, in each next time moment, the S value does not attain its maximum typical for the inlet layers, since some part of the vanadium is already in the crystal phase. Therefore, the crystallization front spreads out, and its movement decelerates with time. Thus at its greatest, at $t = 12$ min, nuclei generation rate is by two orders of magnitude lower than I_{max}, and at $t = 20$ min, it is lower by three orders of magnitude. Eventually, the number of forming nuclei is so low that nuclei must grow to very large size to remove the supersaturation, required for the further front movement. However, the walls of support pores may limit this growth. Thus, in fine pores crystallization may stop at the stage when supersaturation is still rather high. As a result, front movement stops completely, and catalyst activity becomes constant.

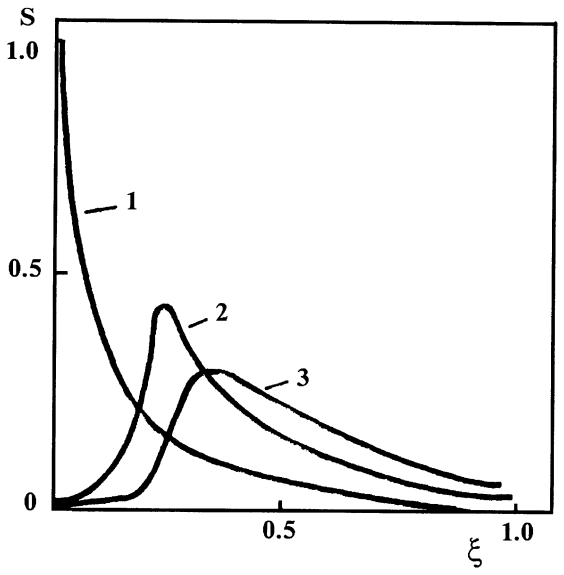

Fig. 7. Calculated supersaturation profile along catalyst bed at time moments (min): 0 (1), 12 (2), 20 (3).

A high sensitivity of nuclei generation rate to supersaturation explains the experimentally observed dynamics of generation rate and front movement, its dependence on the active component composition, porous structure, size of catalyst particles, and catalyst prehistory.

6.1. Effect of chemical composition of active component

Experiment shows that phase transition dynamics can be influenced by a promoting element, its amount and thus atomic ratio between vanadium and promoter. According to our concept, the explanation is as follows.

If atomic ratio K/V increases at a constant vanadium content in the catalyst, active component melt volume increases proportionally, and vanadium concentration in the melt decreases. If other conditions are the same, in the sample with K/V = 6 supersaturation with V^{4+} is twofold lower than in the sample with K/V = 2.7. A twofold decrease of S decreases nuclei generation rate by 3–4 orders of magnitude. As a result, crystallization is less intensive, and thus the front is slower moving in the sample with higher ratio K/V.

At the same ratio M/V samples with cesium are far more stable than samples with potassium (see Fig. 2). We refer to studies [22–24] considering the stability of pyrosulfates of alkaline metals. SO_3 solubility in the active component melt (Henry constant) increases in the order Li, Na, K, Rb, Cs. This means that in the same series, the reduced vanadium portion decreases. Therefore, Cs-containing catalyst should be more resistant to reduction, and thus more stable.

According to the above-mentioned dependence, Na-containing samples should be less resistant to crystallization than K-containing ones. Indeed, in Na promoted samples the degree of vanadium reduction is very high, and so they are practically inactive in SO_2 oxidation.

However, samples, where K is partially substituted by Na demonstrate a higher resistance to crystallization than samples containing solely K [19]. ESR spectra analysis shows that in this case, in the presence of Na, a considerable portion of vanadium(IV) stays in the melt, and does not change to crystal phase. Most likely, sodium introduction into the active component increases the solubility (Θ_∞) and thus decreases supersaturation.

6.2. Porous structure effect

As we have already noted support pore size limits the growth of generated nuclei and crystal particles. In wide pores ($r_p \sim 10^3$ nm) nuclei easily grow to large size, and thus supersaturation is completely removed. The front quickly propagates along the bed, deactivating the whole catalyst. According to the Gibbs–Thompson equation (6), a quasi-equilibrium concentration of V^{4+} in the boundary layer of a nucleus with $r \sim 5 \times 10^2$–5×10^3 nm differs from the true equilibrium concentration (solubility Θ_∞) by several percent only. At the same time, if the nucleus radius $r \sim 10$ nm, V^{4+} content in the boundary layer exceeds Θ_∞ by 20-fold. Therefore, in fine pores crystallization may stop at the stage when supersaturation is still rather high. As a result, front movement decelerates, and only the inlet layers of the catalyst bed, which are responsible for the maximum supersaturation, suffer from crystallization. In deeper layers, where S usually is 20–30, the size of critical nuclei is 8–9 nm, and thus is comparable with the radius of support pores. In this case, either there is no phase transition or phase transition goes at a very low rate.

6.3. Effect of catalyst particle size

Phase transition dynamics become far more complex if reaction occurs on large particle under inner diffusion regime. In this case, there are concentration gradients not only along the catalyst bed, but also along the radius of catalyst particles. Vanadium redox state along the particle radius is easily observed visually, since the particle cross-section shows a color change from green at the surface to yellow in the grain center. It is not easy to get crystal phase distribution over a catalyst particle experimentally. Calculations with the above-described mathematical model show that supersaturation at the particle surface exceeds that inside the grain. As a result, we have crystal phase front moving from the grain surface to its center. According to Fig. 8, front profile over the catalyst particle $\delta(\rho)$ is similar the front profile over catalyst bed $\delta(\xi)$.

Therefore, in a bed of large catalyst particles the crystallization front moves in two directions, towards the particle

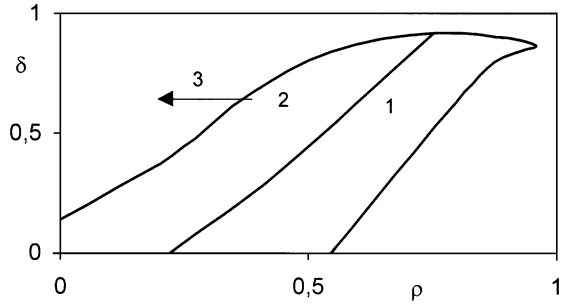

Fig. 8. Calculated profile of crystalline phase along catalyst grain radii at time moments (min): $t = 9$ (1), 27 (2), 39 (3). $\rho = 0$ corresponds to center of particle with $R_{ef} = 2.2$ mm.

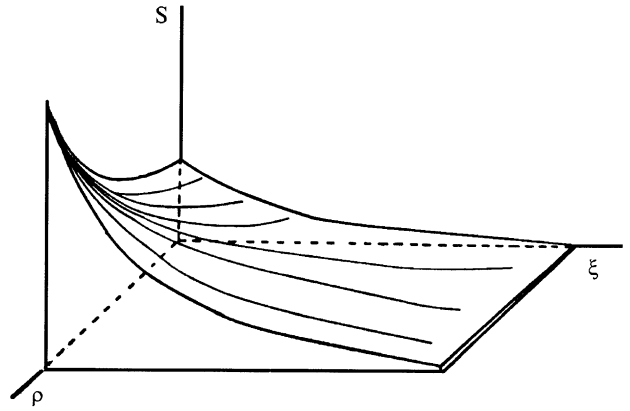

Fig. 9. Calculated surface of bed supersaturation in a system of coordinates fixed in the center of an inlet layer particle with $R_{ef} = 2.2$ mm.

center and also along the bed. Fig. 9 shows the surface of catalyst bed supersaturation in a system of coordinates fixed in the center of the inlet layer particle. Calculations are done at zero time, when there is no crystal phase. In the particle center δ is essentially lower than 1, and thus even in the inlet layers of the bed catalyst is not completely deactivated. At the same time, the front moves further over the particle periphery. As a result, the profile $\delta(\xi)$ for larger particles is more spread out than for small particles. This situation gives a paradoxical result: activity per unit catalyst weight under inner diffusion regime may be higher than that under kinetic regime. This is most probable if the catalyst support has wide pores, where the front moves quickly. This particular situation is realized in sample 2 (Fig. 5). In this case, reaction rate decrease caused by inner diffusion deceleration is less than catalyst activity decrease caused by crystallization.

Figs. 10 and 11 show experimental results and calculation estimates for large catalyst particles. Though experimentally we did not measure the distribution $\delta(\rho)$ but some value

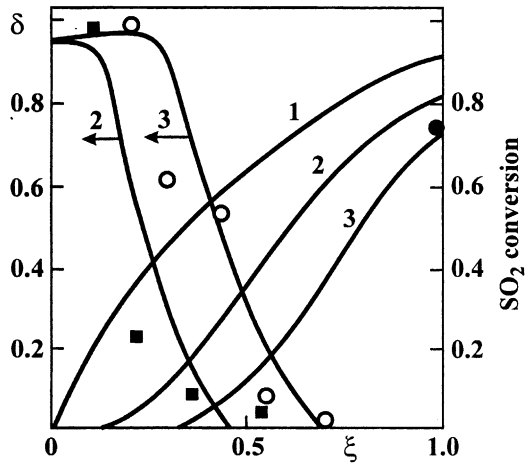

Fig. 10. Crystalline phase amount δ and SO_2 conversion vs. catalyst bed length ξ at time moments (min): 12 (2), 20 (3), line 1 corresponds to $\delta = 0$. Sample 2, fraction 0.5–1.0 mm, $\tau = 0.7$ s. Experimental data (points) and modeling (lines).

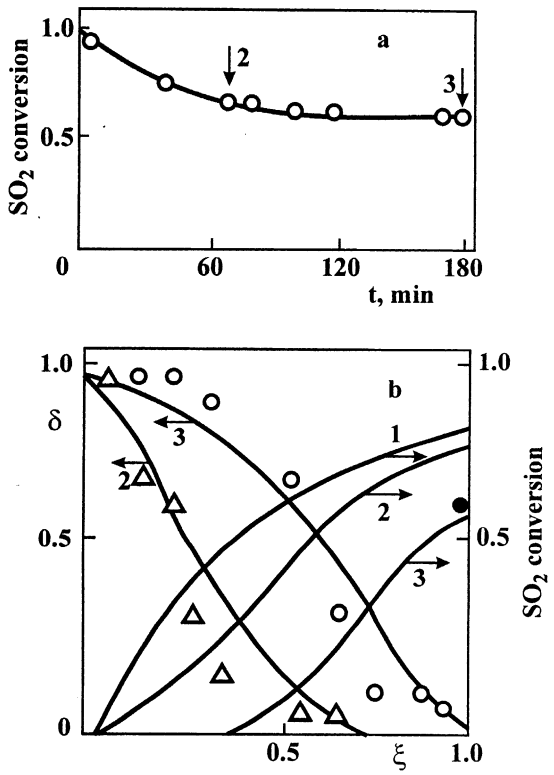

Fig. 11. Time dependence of SO_2 conversion (a) and crystalline phase amount δ vs. catalyst bed length ξ at time moments marked by an arrow (b) (min): 60 (2), 180 (3), line 1 corresponds to $\delta = 0$. Sample 2 in size 5×5, mm, $\tau = 0.7$ s. Experimental data (points) and modeling (lines).

averaged over each particle, nevertheless our simplified model quite accurately reflects the dynamics of phase transition in the bed of industrial catalyst particles and related catalyst activity evolution.

6.4. Prehistory role

The experiment presented in Fig. 6 shows that crystal phase front position is determined not only by the final reaction conditions, but also by the sequence of supersaturation conditions which the catalyst passed through earlier. This effect is revealed as a hysteresis of catalyst activity with respect to temperature and conversion typical for vanadium catalysts.

7. Conclusion

Phase transitions in the active component of vanadium catalysts for sulfuric acid production caused by the crystallization of compounds of vanadium(IV) may significantly influence the fixed bed catalyst activity. Reaction mixture flow through the catalyst bed generates a moving front of crystal phase, whose propagation inside the catalyst bed causes a decrease of sulfur dioxide conversion.

Phase transition peculiarities, crystal phase front generation and dynamics, and decrease in activity are qualitatively and quantitatively described by the suggested mathematical model based on the classic theory of Gibbs–Volmer. The model allows one to predict catalyst behavior, activity evolution along the bed in time in the low temperature zones of industrial apparatuses.

Since phase transition rate and depth depend on the chemical composition of active component and on the porous structure of catalyst support, one can optimize the key parameters of the low temperature catalyst.

Acknowledgements

This study was financially supported by the Russian Foundation for Basic Research (Grant No. 99-03-32425).

References

[1] G.K. Boreskov, L.P. Davydova, V.M. Mastikhin, G.M. Polyakova, ESR studies of vanadium catalysts composition, Dokl. Akad. Nauk SSSR 171 (1966) 648 (in Russian).
[2] B.S. Bal'zhinimaev, S.V. Kozyrev, G.K. Boreskov, A.A. Ivanov, N.P. Belyaeva, V.I. Zaikovskii, Slow relaxation and hysteresis phenomena related to vanadium catalyst activity in sulphur dioxide oxidation, in: Heterogeneous Catalysis, IC SB USSR, Novosibirsk, 1982 (in Russian).
[3] E.V. Gerburt-Geibovich, G.K. Boreskov, Temperature dependence of the rate of sulphur dioxide oxidation on vanadium catalysts, Zh. Fiz. Khim. 30 (1956) 1801 (in Russian).
[4] A.A. Ivanov, G.M. Polyakova, Kinetics and mechanism of sulphur dioxide oxidation on vanadium catalysts, in: Mechanism and Kinetics of Catalytic Processes, IC SB SSSR, Novosibirsk, 1977 (in Russian).
[5] G.K. Boreskov, V.P. Pligunov, Kinetics of contactive SO_2 oxidation, Zh. Pricl. Khim. 6 (1933) 785 (in Russian).
[6] B.S. Bal'zhinimaev, N.P. Belyaeva, A.A. Ivanov, Phase transitions in V_2O_5–$K_2S_2O_7$ melt in sulphur dioxide oxidation, Rasplavy 1 (1987) 92 (in Russian).
[7] J.P. Dun, H.G. Stenger Jr., I.E. Wachs, Oxidation of sulfur dioxide over supported vanadia catalysts: molecular structure–reactivity relationship and reaction kinetics, Catal. Today 51 (1999) 301.
[8] K.M. Eriksen, C.K. Jensen, S.B. Rasmussen, C. Oehlers, B.S. Bal'zhinimaev, R. Fehrmann, ESR spectroscopic characterization of $DeNO_x$ and SO_2 oxidation catalysts and model systems, Catal. Today 54 (1999) 465.
[9] B.S. Bal'zhinimaev, A.A. Ivanov, O.B. Lapina, V.M. Mastikhin, K.I. Zamaraev, Mechanism of sulphur dioxide oxidation over supported vanadium catalysts, Faraday Discuss. Chem. Soc. 87 (1989) 227.
[10] G.I. Petrovskaya, A.A. Ivanov, B.M. Maslennikov, Industrial operating experience of catalysts in manufacture of sulfuric acid, in: Catalysis in Production of Sulfuric Acid, IC SB USSR, Novosibirsk, 1982 (in Russian).
[11] S.V. Kozyrev, B.S. Bal'zhinimaev, G.K. Boreskov, A.A. Ivanov, V.M. Mastikhin, ESR studies of slow relaxations of the rate of sulphur dioxide oxidation on vanadium catalyst, React. Kinet. Catal. Lett. 20 (1982) 53.
[12] A.E. Nielsen, Kinetics of Precipitation, Pergamon Press, Oxford, 1964.
[13] O. Söhnel, J. Nyvlt, Precipitation, in: Fundamentals of Catalysts Production, Nauka, Novosibirsk, 1982 (in Russian).
[14] Ya.B. Zel'dovich, To the theory of new phase generation. Cavitation, Zh. Exper. i Teoret. Fiz. 12 (1942) 525 (in Russian).

[15] V.D. Mesherayakov, G.K. Boreskov, V.S. Sheplev, A.A. Ivanov, Influence of phase transformations in active component of vanadium catalysts on kinetics of sulphur dioxide oxidation, in: Catalysis in Production of Sulfuric Acid, IC SB USSR, Novosibirsk, 1982 (in Russian).
[16] V.M. Mastikhin, O.B. Lapina, L.G. Simonova, ^{17}O and ^{51}V NMR studies of complex formation in $K_2S_2O_7nV_2O_5$ during catalytic oxidation of SO_2, React. Kinet. Catal. Lett. 26 (1984) 431.
[17] B.S. Bal'zhinimaev, N.P. Belyaeva, A.A. Ivanov, Kinetics of dissolution of inactive crystalline phase in vanadium catalysts for SO_2 oxidation, React. Kinet. Catal. Lett. 29 (1985) 465.
[18] S.I. Reshetnikov, B.S. Bal'zhinimaev, V.P. Gaevoi, A.A. Ivanov, Mathematical modeling of a fluidized bed reactor taking into account unsteady state of the catalyst, Chem. Eng. J. 60 (1995) 131.
[19] N.P. Belyaeva, B.S. Bal'zhinimaev, L.G. Simonova, V.I. Zaikovskii, A.A. Ivanov, G.K. Boreskov, Influence of porous support structure and active component composition on deactivation of vanadium catalysts in SO_2 oxidation, React. Kinet. Catal. Lett. 30 (1986) 9.
[20] M. Volmer, Kinetics of New Phase Generation, Nauka, Moscow, 1972.
[21] A.A. Ivanov, B.S. Bal'zhinimaev, New data on kinetics and reaction mechanism for SO_2 oxidation over vanadium catalysts, React. Kinet. Catal. Lett. 35 (1987) 81.
[22] G.H. Tandy, J. Appl. Chem. 6 (1956) 68.
[23] V.I. Spitsynand, I.E. Mikhailenko, J. Inorg. Chem. 2 (1957) 2416.
[24] H. Flood, T. Forland, The acidic and basic properties of oxidates. II. The thermal decomposition of pyrosulfates, Acta Chim. Scand. 1 (1947) 781.